A R C H I V E S O F M E T A L L U R G Y A N D M A T E R I A L S
Volume 60 2015 Issue 1
DOI: 10.1515/amm-2015-0079

E. SKOŁEK*, S. MARCINIAK*, P. SKOCZYLAS**, J. KAMIŃSKI*, W.A. ŚWIĄTNICKI*

NANOCRYSTALLINE STEELS' RESISTANCE TO HYDROGEN EMBRITTLEMENT

ODPORNOŚĆ NA KRUCHOŚĆ WODOROWĄ STALI NANOKRYSTALICZNYCH

The aim of this study is to determine the susceptibility to hydrogen embrittlement in X37CrMoV5-1 steel with two different microstructures: a nanocrystalline carbide-free bainite and tempered martensite. The nanobainitic structure was obtained by austempering at the bainitic transformation zone. It was found, that after hydrogen charging, both kinds of microstructure exhibit increased yield strength and strong decrease in ductility. It has been however shown that the resistance to hydrogen embrittlement of X37CrMoV5-1 steel with nanobainitic structure is higher as compared to the tempered martensite. After hydrogen charging the ductility of austempered steel is slightly higher than in case of quenched and tempered (Q&T) steel. This effect was interpreted as a result of phase composition formed after different heat treatments.
Keywords: carbide-free bainite, tool steel, austempering, hydrogen embrittlement

Celem pracy było określenie wrażliwości na kruchość wodorową stali X37CrMoV5-1 o dwóch różnych mikrostrukturach: nanokrystalicznego bainitu bezwęglikowego i odpuszczonego martenzytu. Struktura nanobainityczna została otrzymana w wyniku procesu hartowania izotermicznego w zakresie przemiany bainitycznej. Zaobserwowano, że po procesie katodowego nasycania wodorem oba typy mikrostruktury wykazują zwiększenie granicy plastyczności i znaczący spadek plastyczności. Wykazano jednak, że odporność na kruchość wodorową stali X37CrMoV5- 1o strukturze nanobainitycznej jest lepsza w porównaniu do stali o strukturze martenzytu odpuszczonego. Po katodowym nasycaniu wodorem plastyczność stali hartowanej izotermicznie jest nieznacznie wyższa niż w przypadku stali hartowanej i odpuszczanej (Q&T). Zjawisko to zostało zinterpretowane jako wynik składu fazowego wytworzonego podczas różnych obróbek cieplnych.

1. Introduction

At present steels are still the most widely used structural material, that's why there are many research with objective to increase their strength. However, with increasing the strength of material, there is a tendency to increase the susceptibility to hydrogen embrittlement [1-3]. Absorption of hydrogen into steel causes some irreversible changes in the material microstructure [4-9]. These changes are different in various phases present in steel because the hydrogen interact in various manner each phase of steel. The diffusivity of hydrogen in ferrite is much higher than in austenite, whereas its solubility is higher in austenite [7,10]. The presence of hydrogen leads to the strong increase of dislocations density in ferrite and to formation of stacking faults in austenite [4,5]. With increasing hydrogen content in steel these effects increase. Moreover the phase transformations may appear such as for example the martensitic transformation in austenite [5-7]. All observed changes reduce the possibility of plastic accommodation of stresses which are generated by application of external forces to the steel element. Thus, under the effect of stresses the micro-cracks appear in ferrite and on intercrystalline boundaries [7-9]. Therefore the increase of hydrogen concentration may lead to the so called hydrogen embrittlement which is manifested by delayed hydrogen cracking, by significant decrease in plasticity of steel and by reduced toughness [7-9]. The susceptibility of steel to hydrogen embrittlement depends on the chemical composition of steel, its microstructure, phase composition and internal stresses [1,7,8,11-15].

It was observed that steels with higher strength, as for example martensitic steels, are more susceptible to hydrogen embrittlement [11-14]. This is due to the high density of defects which interact strongly with hydrogen atoms. Moreover the high strength steels have low susceptibility of stress relaxation. A question arises if all strengthening mechanisms promote the hydrogen embrittlement? In particular, what is the effect of hydrogen on high strength steels with nanocrystalline structure?

In recent years a new type of bainitic steels with nanocrystalline structure which provides a high strength was developed [16-21]. These steels have the structure of carbide-free bainite which is composed of nanometric ferrite plates separated by thin layers of retained austenite. The high ductility and toughness of these steels are due to relatively

* WARSAW UNIVERSITY OF TECHNOLOGY, FACULTY OF MATERIALS SCIENCE AND ENGINEERING, 141 WOLOSKA STR., 02-507 WARSAW, POLAND
** WARSAW UNIVERSITY OF TECHNOLOGY, FACULTY OF PRODUCTION ENGINEERING, 85 NARBUTTA STR., 02-524 WARSAW, POLAND

high content of retained austenite, up to 50%. We have recently developed a heat treatment of X37CrMoV5-1 hot work tool steel which allowed us to obtain a nanocrystalline structure composed of carbide free bainite with retained austenite in form of layers and small blocks [19].

The aim of the work was to investigate and compare the effect of hydrogen on the mechanical properties of X37CrMoV5-1 steel with the nanobainitic structure and the same steel with the conventional structure of tempered martensite.

2. Experimental methods

The X37CrMoV5-1 tool steel of the following chemical composition: C-0,37% Si-1,01% Mn-0,38% Cr-4,91% Mo-1,2% V-0,34% Ni-0,19% was subjected to austenitizing at the temperature of 1030°C for 15 min., and then was cooled down to the temperature of 300°C, annealed at that temperature in a liquid tin alloy for the time allowing to finish the bainite transformation. After isothermal quenching the samples were cooled down in the air. A second set of samples was submitted to the conventional heat treatment dedicated for this steel consisting on martensitic quenching in oil and tempering at 585°C for 2 h. The hardness of the austempered steel is similar to the hardness of the steel quenched and tempered (Q&T) and it amounts to 510 and 550 HV2 respectively.

The microstructure of heat treated samples were investigated by transmission electron microscopy (TEM) using STEM JEOL 1200EX microscope. TEM observations were carried out in the bright field (BF) and dark field (DF), using the reflections coming from various phases. In order to characterise the phase composition and the microstructure (grain size, content of phases) the methods of the stereological analysis were applied.

The width of ferrite and austenite grains visible on the TEM images was determined from the formula:

$$d = \frac{2}{\Pi} L \tag{1}$$

where d is actual dimension of the microstructure element, L – dimension of this element measured on TEM image [22].

Volume fractions of the phases were calculated with the assumption that the volume content of a given phase is equivalent to its share in the microstructure image plane. A number of secant lines of the length l was applied to images of microstructure intersecting with specific phase n-times. The following formula was used to calculate phase composition:

$$V_v = \frac{\Sigma c_{ik}}{l} \tag{2}$$

where $\sum c_{ik}$ is the sum of the widths of all intersections of the secant line l with a given phase, l – length of the secant line.

In order to investigate the hydrogen effect on the mechanical properties of steel the tensile tests were performed on both kinds of samples before and after hydrogen charging.

The static tensile tests before hydrogen charging were performed on the samples with diameter of 6 mm, in accordance to the standard PN-EN 10002-1:2004 [23] using Zwick/Roell Z250 strength machine with the extensometer. The samples were strained with the strain rate of $10.6\times10^{-4}s^{-1}$.

Cathodic hydrogen charging process was performed on the tensile samples with a diameter of 2.1 mm for the time of 112 hours in 0,1M H_2SO_4 environment with the addition of As_2O_3 (10 ml As_2O_3 per l000 ml H_2SO_4) as the promoter of hydrogen entry (hydrogen recombination poison). The time needed for complete hydrogen charging of tensile samples of the X37CrMoV5-1 steel was estimated on the basis of the hydrogen diffusion coefficient in pure iron [24] and in two-phase X2CrNiMoN23-5-3 austenitic-ferritic steel [11], assuming winding paths of hydrogen diffusion in steel. During the process of hydrogen charging, the density of current $20mAcm^{-2}$ was applied.

After 96 hours of completing the cathodic hydrogen charging process the samples were submitted to the static tensile tests. These tests were performed on an Intron model 1115 tensile test machine with the measurement head up to 100 kN. The initial applied strain rate was equal to $2.8\times10^{-4}s^{-1}$. In this case samples with a diameter of 2.1 mm were used.

Fracture surfaces observations were performed with the use of SEM.

3. Results and discussion

As a result of conducted austempering treatment an extremely fine structure was developed, with a needle-shaped character. Detailed identification of phases performed by means of a transmission electron microscope revealed that steel microstructure is composed of carbide-free bainitic plates separated by the layers of retained austenite. The average content of bainitic ferrite in the sample amounts to 55±3%, the rest is a retained austenite with some amount of the martensite. The bainitic ferrite plates have an average thickness of 89 nm±6 nm and the austenite layers of 31 nm±2 nm (Fig. 1).

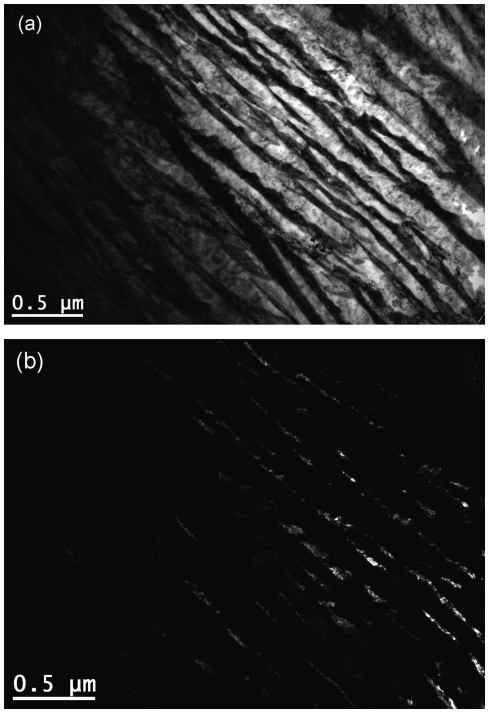

Fig. 1. Microstructure of X37CrMoV5-1 steel after austempering at 300°C: (a) bright field image and (b) dark field image for austenite reflection

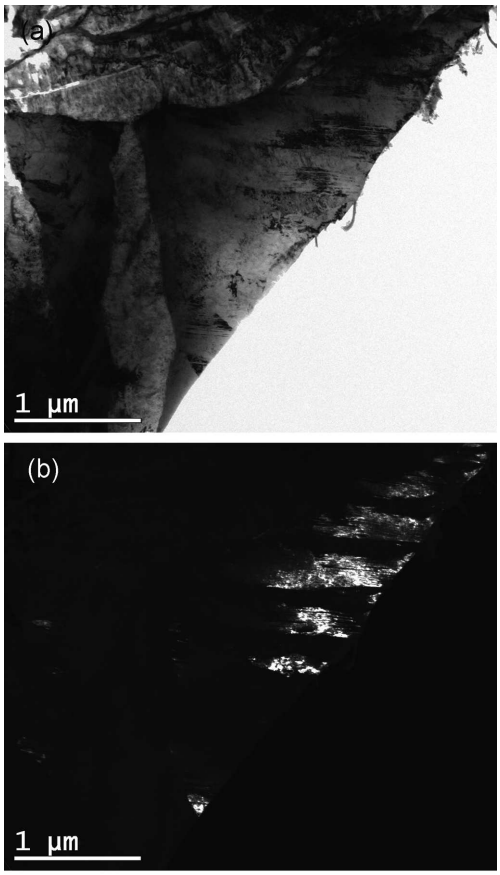

Fig. 2. The block of austenite partially transformed to martensite in X37CrMoV5-1 after austempering at 300°C: (a), bright field image, (b) dark field image for ferrite reflection

The retained austenite appears also in form of blocks. The cross section area of blocks vary from 0.13 μm^2 to 4.33 μm^2 (Fig. 2). It was revealed that the blocks of retained austenite were partially transformed into martensite, that is why it was measured the content of the ferrite and the content of austenite/martensite phases mixture. There were also numerous midribs observed.

The period of 96 hours between the end of cathodic hydrogen charging and the start of the tensile strength tests, was necessary to desorption of the diffusive hydrogen from the sample. Mainly hydrogen trapped at defects could remain in the steel. Fig. 3 presents the tensile properties of 37CrMoV5-1 steel after austempering and quenching and tempering treatments before and after hydrogen charging. Before the hydrogen charging the yield strength ($R_{0.2}$) for steel with a nanobainitic structure is 734 MPa and for quenched and high tempered steel amounts to 1403 MPa. Tensile strength is similar after both types of heat treatment and amounts to 1763 and 1700 MPa, respectively. The total elongation reaches 16.6% in the case of samples subjected to isothermal quenching and 13.1% in case of Q&T samples. After hydrogen charging both kinds of samples show a strong decrease of plastic properties, however the decrease of ductility is smaller in nanobainitic samples. Hydrogenation leads also to an increase in yield strength in both kinds of samples. The value of the yield strength increased to 1056 for austempered sample and to 1512 MPa for Q&T sample. This can be due to the increased density of defects induced by hydrogen during cathodic charging in ferrite and in austenite as it was shown in our previous works [4,5,7]. The tensile strength slightly decreases, but it is still relatively high and similar for both kinds of treatment – about 1488 MPa for the nanobainitic structure and about 1573 MPa for tempered martensite. The decrease of strength observed in both samples results from reduced elongation.

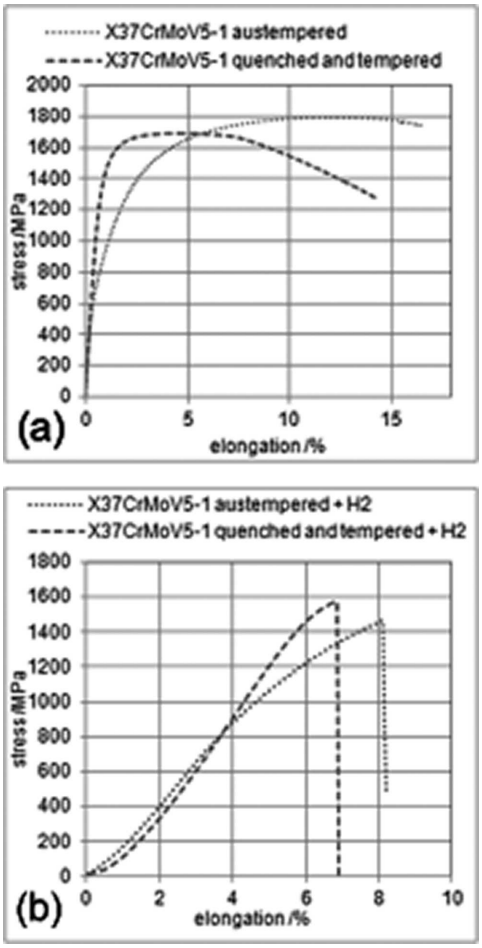

Fig. 3. Tensile curves of the X37CrMoV5-1 steel after austempering and quenching and tempering treatments before (a) and after (b) hydrogen charging

The mechanical properties of steel after and before the hydrogen charging are summarised in Table 1. Hydrogen unfavourably influences the plasticity of steel, regardless of thermal treatment. After hydrogen charging, the plasticity decreases significantly compared to samples before hydrogen charging. This effect is dramatic in the case of samples with tempered martensite, for which the total elongation and uniform elongation initially equal to 13.1 and 4.1 respectively, decrease after hydrogenation to a value of 0.7%. It means that Q&T samples are extremely brittle after hydrogenation. The decrease of plasticity is slightly smaller in case of austempered steel: the uniform as well as total elongation of austempered steel after hydrogenation is 1.8%. This value is 2.6 times higher than in the case of Q&T steel samples. It means that the nanobainitic 37CrMoV5-1 steel is less susceptible to the hydrogen embrittlement than steel with tempered martensite.

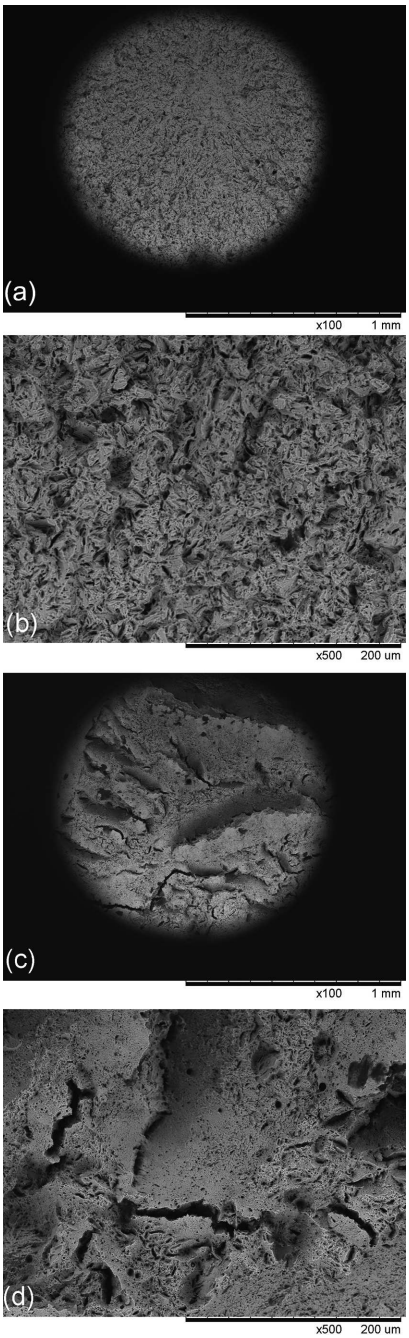

Fig. 4. Fracture surfaces of steel samples before hydrogen charging after austempering (a), (b) and quenching and tempering (c), (d) treatment

After tensile tests performed before and after hydrogen charging the fracture surfaces were observed by means of SEM (Fig. 4, 5).

Before hydrogen charging in both tensile tested steel samples fracture surfaces are similar with a shear character. The surface is deformed, with many ”craters” and elongated and thinned peaks of the phase with a greater plasticity. In the fractured steel samples subjected to Q&T process, many secondary cracks were observed (Fig. 4c,d). Fractures of the samples after austempering treatment are more homogeneous (Fig. 4a,b).

TABLE 1
Characteristics mechanical parameters of X37CrMoV5-1 steel after austempering and quenching and tempering treatment before and after hydrogen charging

	before hydrogen charging		after hydrogen charging	
	austempered	Q&T	austempered	Q&T
$R_{0.2}$/MPa	734±8	1403±47	1056±44	1512
R_m/MPa	1763±55	1700±62	1488±58	1573
A_T/%	16.6±1.4	13.1±1	1.8±0.3	0.7
A_u/%	12.1±0.6	4.1±0.2	1.8±0.3	0.7

Fracture surfaces of tensile tested samples after hydrogen charging, have a separating and brittle character, with a small value of reduction of area at fracture. The surfaces of cracking are mat and oriented perpendicularly to the direction of loading. The SEM observations revealed that the fracture surface of austempered steel have slightly plastic character. Fracture surface is smooth, with some secondary cracks (Fig. 5a,b). In the case of Q&T steel fracture surface is heterogeneous – there are areas typical for brittle breaks with many cracks (Fig. 5e) and also areas with slightly plastic character containing craters that may arise as a result of pull out hard particles or fragments of the material (Fig. 5d).

The observed difference in susceptibility to hydrogen degradation in both kinds of steel samples may results from several factors, mainly from the phase composition. Steel 37CrMoV5-1 after austempering treatment contains about 55% of bainitic ferrite and 45% of retained austenite with small amount of martensite, so that it can be considered as a dual-phase steel. In previous works on hydrogen embrittlement of dual phase steels [7,10,25,26] it has been shown, that the diffusion coefficient of hydrogen in austenite is several orders of magnitude smaller than in the ferrite and the solubility of hydrogen – an order of magnitude larger than in ferrite. Thus, austenite can absorb much more hydrogen than ferrite. Due to the low mobility, the hydrogen is trapped in austenite. Moreover, in dual phase steels austenite also increases tortuosity of the hydrogen diffusion paths in the structure [25]. In nanobainitic steel, retained austenite surrounds the ferrite plates on all sides, thus it can easily close the diffusion path through the ferrite grains, and inhibit propagation of hydrogen induIn nanobainitic steel samples the grain size is small, and thus the surface area of intergranular boundaries, which are the hydrogen traps, is high [26]. According to the work of Rivera-Díaz-del-Castillo [28] the high density of hydrogen traps can immobilise the diffusive hydrogen in steel microstructure, and by this way led to a reduction of the embrittlement effects. The grains refinement in nanobainitic steels may therefore, be another factor affecting the resistance to hydrogen embrittlement.

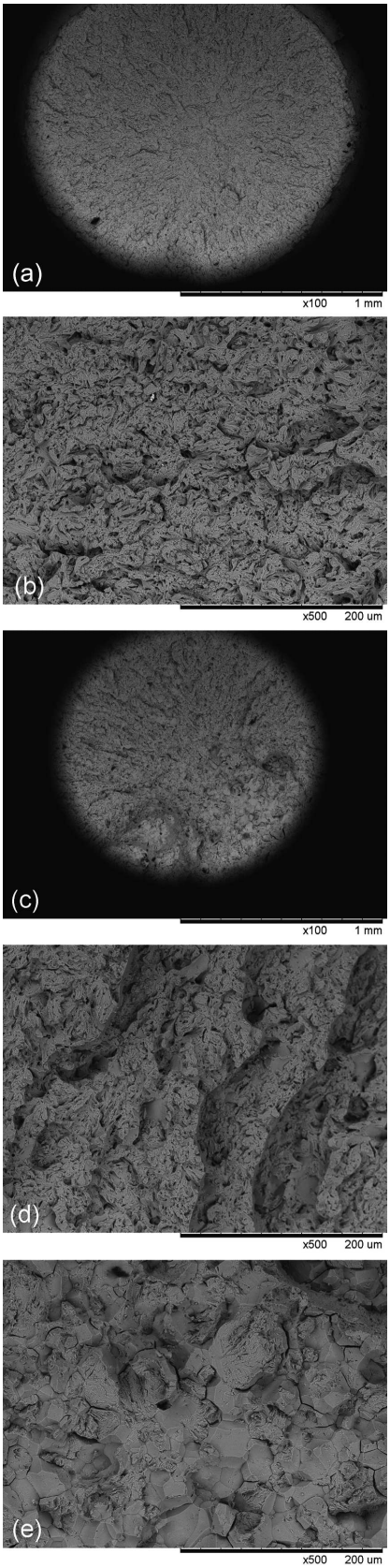

Fig. 5. Fracture surfaces of steel samples after hydrogen charging after austempering (a), (b) and quenching and tempering (c), (d), (e) treatment

4. Summary

Tensile tests performed on X37CrMoV5-1 steel samples with two different microstructures submitted previously to hydrogen charging indicate a strong decrease of ductility during tensile tests in both kinds of samples. The fracture surface observations of tensile tested samples confirm the hydrogen embrittlement effects.

The decrease in ductility is higher in the case of tempered martensite, than in the case of nanobainitic structure. The lesser susceptibility to hydrogen embrittlement of the nanobainitic structure was interpreted as a result of high volume fraction of retained austenite and high density of intergranular and interphase boundaries which constitute the effective hydrogen traps. Thus, it can be assumed that the presence of high density of grain and interphase boundaries in nanocrystalline steels is not harmful factor from the viewpoint of hydrogen embrittlement. On the contrary the interphase boundaries ferrite/austenite may reduce the hydrogen embrittlement effects.

It is concluded, that the nanobainitic structure with high content of retained austenite exhibit slightly higher resistance to hydrogen embrittlement, in comparison to the steel with tempered martensite and higher grain size.

Acknowledgements

The results presented in this paper have been obtained within the Dean Grant no. 504M/1090/70/000 and the project "Production of nanocrystalline steels using phase transformations" – NANOSTAL (contract no. POIG 01.01.02-14-100/09 with the Polish Ministry of Science and Higher Education), co-financed by the European Union from the European Regional Development Fund within Operational Programme Innovative Economy 2007-2013.

REFERENCES

[1] L. Tau, S.L.I. Chan, C.S. Shin, Corrosion Science **38**, 2049-2060 (1996).
[2] M. Beghini, G. Benamati, L. Bertini, I. Ricapito, R. Valentini, Journal of Nuclear Materials **288**, 1-6 (2001).
[3] G. Wang, Y. Yan, J. Li, J. Huang, Y. Su, L. Qiao, Corrosion Science **77**, 273-280 (2013).
[4] A. Głowacka, W.A. Świątnicki, Journal of Alloys and Compounds **356-357**, 701-704 (2003).
[5] A. Głowacka, W.A. Świątnicki, E. Jezierska, Journal of Microscopy **223**, 282-284 (2006).
[6] A. Głowacka, M.J. Wozniak, W.A. Swiatnicki, Journal of Alloys and Compounds **404-406C**, 595-598 (2005).
[7] W. Świątnicki, Proceedings of 2008 'International Hydrogen Conference – Effects of Hydrogen on Materials, Jackson Lake Lodge, Grand Teton National Park, Wyoming, USA, September, 2008, eds. B. Somerday, P. Sofronis, R. Jones, ASM International, 155-162 (2009).
[8] T. Zakroczymski, A. Głowacka, W.A. Świątnicki, Corrosion Science **47**, 1403-1414 (2005).
[9] B. Gołębiowski, W.A. Świątnicki, M. Gasperini, Journal of Microscopy **237**, 352-358 (2010).
[10] E. Owczarek, T. Zakroczymski, Acta Materialia **48**, 3059-3070 (2000).
[11] W.C. Luu, J. K. Wu, Corrosion Science **38**, 239-245 (1996).
[12] U. Hadam, T. Zakroczymski, International Journal of Hydrogen Energy **34**, 2449-2459 (2009).

[13] J. Ćwiek, K. Nikiforov, Materials Science **40**, 831-836 (2004).
[14] J. Ćwiek, Journal of Achievements in Materials and Manufacturing Engineering **37**, 193-212 (2009).
[15] M. Sozańska, J. Sojka, P. Betakova, C. Dagbert, L. Hyspecka, J. Galland, M. Tvrdy, Materials Characterization **46**, 239-243 (2001).
[16] H.K.D.H. Bhadeshia, Proc. R. Soc. A **466**, 3-18 (2010).
[17] H.K.D.H. Bhadeshia, Mater. Sci. Eng. A **481-482**, 36-39 (2008).
[18] C. Garcia-Mateo, F.G. Caballero, Mater. Trans. **46**, 1839-1846 (2005).
[19] W.A. Świątnicki, K. Pobiedzińska, E. Skołek, A. Gołaszewski, Sz. Marciniak, Ł. Nadolny, J. Szawłowski, Materials Engineering (Inżynieria Materiałowa) **6**, 524-529 (2012).
[20] J. Dworecka, K. Pobiedzińska, E. Jezierska, K. Rożniatowski, W. Świątnicki, Materials Engineering (Inżynieria Materiałowa) **2**, 109-112 (2014).
[21] W. Burian, J. Marcisz, B. Garbarz, L. Starczewski, Archives of Metallurgy and Materials **59**, 1211 (2014).
[22] L.C. Chang, H.K.D.H. Bhadeshia, Materials Science and Technology **11**, 874-881 (1995).
[23] 'Metale – Próba rozciągania' – Część 1 'Metoda badania w temperaturze otoczenia', PN-EN 10002-1:2004.
[24] Z. Wolarek, T. Zakroczymski, Acta Materialia **52**, 2637-2643 (2004).
[25] T. Zakroczymski, E. Owczarek, Acta Materialia **50**, 2701-2713 (2002).
[26] A. Turnbull, R.B. Hutchings, Mater. Sci. Eng. **A177**, 161-171 (1994).
[27] Shyan-Liang Chou, Wen-Ta Tsai, Mater. Sci. Eng. **A270**, 219-224 (1999).
[28] P.E.J. Rivera-Díaz-Del-Castillo, Metallurgical and Materials Transactions A **44**, 4542-4550 (2013).

Received: 20 March 2014.